

Fluid flow generates bacterial conjugation hotspots by increasing the rate of shear-driven cell-cell encounters.

Matti Zbinden,¹ Jana S. Huisman,² Roman Stocker,¹ and Jonasz Słomka¹

¹*Institute of Environmental Engineering, Department of Civil, Environmental and Geomatic Engineering, ETH Zurich, Zurich, Switzerland*

²*Department of Physics, Massachusetts Institute of Technology, Cambridge, Massachusetts, USA*

(Dated: October 10, 2024)

Conjugation accelerates bacterial evolution by enabling bacteria to acquire genes horizontally from their neighbors. Because plasmid donors must physically connect with recipients to allow plasmid transfer, environmental fluid flows may increase conjugation rates by increasing cell-cell encounters through mixing driven by fluid shear, which creates relative movement between donors and recipients. However, existing experimental assays do not directly control cell-cell encounters, which hinders the establishment of a connection between the population-level conjugation rate and the microscale mechanisms that bring cells together. Here, we performed conjugation experiments between *E. coli* bacteria, varying the shear flow to control the rate of cell-cell encounters. We discovered that the conjugation rate increases with shear until it peaks at an optimal shear rate ($\dot{\gamma} \approx 10^2 \text{ s}^{-1}$), reaching a value five-fold higher than the baseline set by diffusion-driven encounters. This optimum marks the transition from a regime in which shear promotes conjugation by increasing the rate of cell-cell encounters to a regime in which shear disrupts conjugation. Fluid flows are widely present in aquatic systems, gut, and soil, and our results indicate that fluid shear could induce hotspots of bacterial conjugation in the environment.

Bacteria evolve rapidly because they share genes not only vertically, from parents to offspring, but also horizontally, between cells that come in contact with each other [1–3]. Up to 25% of the bacterial genome consists of horizontally acquired genes [4]. Along with transformation (direct DNA uptake) and transduction (virus-mediated DNA transfer), conjugation is a major horizontal gene transfer pathway [3], takes place in diverse environments [5, 6], and is strongly implicated in the global spread of antimicrobial resistance [7]. Conjugation starts with an encounter between a plasmid donor and a recipient, followed by a contact mediated by a conjugative pilus, a type-IV secretion system (T4SS) that transports a single-stranded DNA copy of the plasmid from the donor to the recipient cell [8] within approximately ten minutes [9, 10]. Upon receiving the plasmid, the recipient becomes a transconjugant, capable of spreading the plasmid further at a rate that depends on cell-cell encounters.

Different environments present plasmid donors with vastly different encounter rates. Environmental fluids bring cells together through mixing induced by fluid shear, which creates a relative movement between the donors and recipients, or through diffusion when a flow is absent [11]. For example, the surface ocean generates more cell-cell encounters due to the combined effects of strong turbulence [12] and elevated cell densities [13] than the quiescent deeper ocean. Similarly, gut peristalsis [14] and preferential flow paths in porous media [15] generate high levels of intermittent mixing with the associated shear rates spanning orders of magnitude [15, 16]. To date, however, the impact of microscale encounters on

conjugation has not been directly explored.

Decades of study have shown that the success of conjugation depends on many environmental and biological factors [17, 18]. Conjugation is typically quantified by measuring the conjugation rate η [19–21]. Over a mating duration t_m where cell growth can be neglected, it is computed as [20–23]

$$\eta \approx \frac{c_T(t_m)}{t_m c_D(0) c_R(0)}, \quad (1)$$

where $c_D(0)$, $c_R(0)$ are the initial concentrations of donor and recipient cells, and $c_T(t_m)$ is the endpoint concentration of transconjugants. This formulation can be extended to account for cell growth using endpoint formulae [19–21, 24]. Observed conjugation rates vary by more than ten orders of magnitude and depend on plasmid type and size, pilus type, phylogenetic relatedness of donor and recipient, and the environment (temperature, media type, in liquid or on the surface) [18]. Previous experiments suggested an important role for fluid shear in controlling conjugation efficiency [25–27]. However, while fluid shear may act to increase the conjugation rate by increasing cell-cell encounters, it may also hamper the plasmid transfer by disrupting the mating pairs. Separating these two opposing effects of shear in conventional laboratory shakers is hard, because they create flows that are difficult to control. Consequently, it is challenging to link laboratory experiments with the potential of various environments to act as bottlenecks or hotspots of conjugation, especially since environmental flows present cells with vastly different encounter conditions.

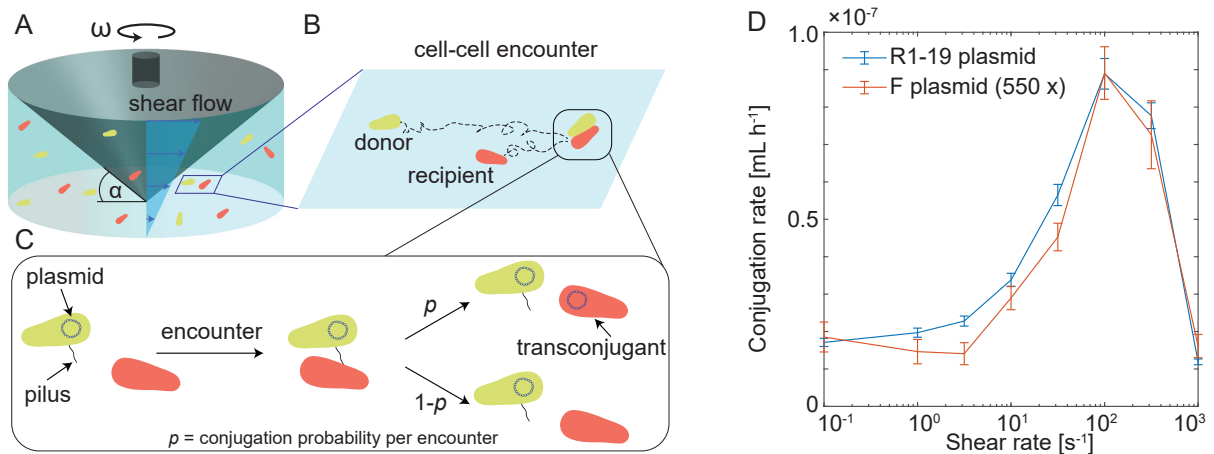


FIG. 1: Bacterial conjugation rate peaks at an optimal shear rate. **A**, The schematic shows a suspension of plasmid donors and recipients mixed in a cone and plate rheometer. The cone geometry generates a shear flow throughout the sample, which is controlled by the rotation rate of the cone. The angle α of the cone with the horizontal plate is exaggerated for visualization purposes. **B**, Cell-cell encounters are generated by two mechanisms in liquid: (i) the shear flow, which induces relative movement between cells occupying slightly different vertical positions, and (ii) simple diffusion (Brownian motion). The encounter rate is controlled in the sample because the applied shear rate is tightly controlled. **C**, A schematic of the conjugation process in which an encounter between donor and recipient leads to conjugation with probability p . **D**, The observed conjugation rate η for two *E. coli* strains (TB04 for donors; NCM Δ mot for recipients) sharing a conjugative plasmid (pR1-19, blue, or F, orange) as a function of the applied shear rate $\dot{\gamma}$. The data represents an average and the error bars standard errors for $n = 4$ independent ramp-up/ramp-down experiments for each plasmid (Methods). Upon rescaling (550x) of the rate for the F plasmid, both plasmids show very similar shear responses, with the conjugation rate peaking at an optimal shear rate about five-fold higher than the baseline rate.

Here, we introduce a new assay to study quantitatively the effect of flow on the conjugation rate, separate the encounter stage of conjugation from plasmid transfer, and predict plasmid transfer rates in environmentally relevant flows. Using a cone and plate rheometer, we expose a suspension of plasmid donors and recipients to varying shear flows and study how the shear rate impacts the conjugation rate. We discover that, as the shear rate increases, the conjugation rate increases at first, reaches a maximum, and then decreases. At the optimal shear rate, the conjugation rate is enhanced five-fold over the no-flow case, in which Brownian motion alone drives conjugation. We explain the presence of an optimal shear rate by modeling the effect of shear on the encounter rate between donor and recipient cells, together with a detrimental effect of shear at the highest shear rates, due to either the encounter duration being too short to enable mating pair formation or the shear forces obstructing mating. Our experimental results indicate that flow in aquatic, gut, and soil environments could locally increase conjugation rates. As an example, we predict that the ocean surface layer, particularly breaking waves, could act as hotspots of conjugation by generating high enough shear to increase cell-cell encounters without impairing conjugation.

Results

To better assess the effect of fluid shear on conjugation rates, we developed a new experimental assay. We used

a cone and plate rheometer as a ‘cell collider’ (Fig. 1). The cone geometry creates a shear flow in the suspension of donors and recipients (Fig. 1A). In this setup, two mechanisms bring cells together: shear flow and diffusion (Fig. 1B). Diffusion generates cell-cell encounters via Brownian motion of both donor and recipient cells. The shear flow generates encounters by creating a relative horizontal velocity $\delta v \sim \delta z \dot{\gamma}$ between cells separated vertically by a small distance δz . Here $\dot{\gamma}$ is the shear rate, which quantifies the velocity gradient.

We model the encounter rate E between donor cells (concentration $c_D(t)$ at time t) and recipient cells (concentration $c_R(t)$ at time t) per unit volume in the rheometer as

$$E = \Gamma c_D(t) c_R(t), \quad (2)$$

where Γ is the encounter kernel, which represents the relative volume swept per unit time by colliding cells [11, 28]. Γ has the same units as the conjugation rate η and explicitly depends on the encounter mechanism. We make the common assumption that shear flow and diffusion generate encounters independently [29], implying that the total kernel is a sum of two separate kernels

$$\Gamma = \Gamma_{\text{shear}} + \Gamma_{\text{diff}}, \quad (3)$$

with [29, 30]

$$\Gamma_{\text{shear}} = \frac{4}{3}(r_{\text{D}} + r_{\text{R}})^3 \dot{\gamma}, \quad (4a)$$

$$\Gamma_{\text{diff}} = 4\pi(D_{\text{D}} + D_{\text{R}})(r_{\text{D}} + r_{\text{R}}), \quad (4b)$$

where r_{D} and r_{R} are the equivalent radii of donor and recipient cells, respectively, D_{D} and D_{R} are their diffusion coefficients, and $\dot{\gamma}$ is the shear rate.

In the rheometer, the baseline shear rate $\dot{\gamma}$ is controlled by the angular speed ω of the rotating cone: $\dot{\gamma} = \omega / \tan \alpha$, where $\alpha = 4^\circ$ is the angle the cone makes with the horizontal plate (Fig. 1A). The cone base diameter is 4 cm, which holds a sample volume of 1.2 mL. Flows in such geometries have been studied in detail both numerically [31] and experimentally [32]. As the angular speed increases, the flow is laminar for shear rates smaller than $\dot{\gamma} \approx 35 \text{ s}^{-1}$, then secondary flows develop, and the flow becomes turbulent for shear rates above $\dot{\gamma} \approx 300 \text{ s}^{-1}$ [32] (SI). The shear rate is thus constant throughout the sample and equal to the baseline shear rate at low shear. As the shear rate increases, an additional shear rate is created by the secondary and turbulent flows. Based on previous numerical simulations [31] and torque measurements [32], we estimate that the additional shear rate becomes comparable with the baseline rate at shear rates around $\dot{\gamma} \approx 60 \text{ s}^{-1}$ and is at most twice the baseline for the highest shear rate studied here ($\dot{\gamma} = 1 \times 10^3 \text{ s}^{-1}$; SI). Throughout the paper, we will use the baseline shear rate ($\dot{\gamma} = \omega / \tan \alpha$) in Eq. (4a). The control of the shear flow achieved in the rheometer is a key feature of our approach since it enables us to control the encounter rate between cells, in contrast to the complex flow in conventional shakers. Our approach is inspired by mixers developed to study phytoplankton coagulation [33] and fertilization in sea urchins [34] based on an oscillating stirring shaft [33] or the Couette cell [34], though these were developed for larger cells ($>10 \mu\text{m}$) and sample volumes ($>10 \text{ mL}$).

The combination of experimentally controlled shear flow and encounter rate theory enables us to separate the encounter stage of conjugation from plasmid transfer. Assuming that each encounter between a donor and recipient cell has a constant probability of p of producing a transconjugant, the conjugation rate will be related to the encounter kernel as (Fig. 1C)

$$\eta = p\Gamma. \quad (5)$$

In particular, $p = 1$ means that every encounter results in conjugation, i.e., the conjugation rate is as high as the encounter rate. In the following, we will set $r_{\text{D}} = r_{\text{R}} = 1 \mu\text{m}$, $D_{\text{D}} = D_{\text{R}} = 0.28 \mu\text{m}^2 \text{ s}^{-1}$, which follows from the Stokes-Einstein formula, $D = k_{\text{B}}T / (6\pi\mu r)$ for the diffusion coefficient of a sphere of radius $r = 1 \mu\text{m}$ in a fluid with dynamic viscosity of water at the experimental temperature $T = 30^\circ \text{C}$ ($\mu = 0.8 \text{ mPas}$); k_{B} is the

Boltzmann constant. The only free parameter remaining to determine the encounter rate is, therefore, the shear rate $\dot{\gamma}$, which we varied in our experiments to study its impact on conjugation.

We performed conjugation experiments with *E. coli* donor (TB204) and recipient (NCM Δmot) cells sharing a conjugative plasmid (pR1-19 resp. F). We prepared donors and recipients at the same optical density ($\text{OD}_{600} = 0.05$ for R1-19; $\text{OD}_{600} = 0.2$ for F) in LB medium and then mixed them in 1:1 proportions. The exact concentrations were determined by counting cells in a hemacytometer under a microscope before each experiment (average concentrations $c_{\text{D}} = 1.49 \times 10^7 \text{ mL}^{-1}$ and $c_{\text{R}} = 1.05 \times 10^7 \text{ mL}^{-1}$ for R1-19 and $c_{\text{D}} = 4.93 \times 10^7 \text{ mL}^{-1}$ and $c_{\text{R}} = 4.02 \times 10^7 \text{ mL}^{-1}$ for F; Methods, SI). We used low cell concentrations to minimize the chance of non-binary collisions (e.g., between three cells) while maintaining reproducible conjugation yield. We then exposed the donor-recipient mixture (1.2 mL of sample volume) to a constant shear flow in the rheometer for $t_{\text{m}} = 30 \text{ min}$ at constant temperature $T = 30^\circ \text{C}$, after which we sampled cells for analysis (Methods). To count transconjugants, we used the time-to-threshold method [23], whereby a subsample is diluted in a selective medium, promoting only the growth of transconjugants until a threshold optical density value. The time to reach the threshold is then used to back-calculate the initial transconjugant concentration in the subsample ($c_{\text{T}}(t_{\text{m}})$ in Eq. 1) using a predetermined calibration curve. As an additional control for selection, our cells were chromosomally tagged with fluorescence markers (Methods). We then computed the conjugation rate η according to Eq. (1). To measure across all shear rates for the same biological sample, we conducted sequential experiments: we changed the shear rate from low to high in two experiments and from high to low in two other. Each such sweep constituted eight 30-minute-long conjugation experiments using aliquots from the same bacterial cultures. Aliquots of donors and recipients were put at $T = 4^\circ \text{C}$ to suppress cell growth while not in use. Comparing the up and down sweeps revealed no significant impact of the sweep order on the measured conjugation rates (SI).

We found that, as a function of shear rate, the conjugation rate η increases from a plateau at low shear rates ($\dot{\gamma} < 1 \text{ s}^{-1}$) to a maximum at a critical shear rate of $\dot{\gamma} \approx 10^2 \text{ s}^{-1}$, and then decreases again (Fig. 1D). The peak conjugation rate is approximately five times higher than the plateau at low shear rate. While the F plasmid overall exhibited a lower conjugation rate than R1-19, multiplying the values of the conjugation rate for the F plasmid by a constant factor ($550\times$) shows that it exhibits a very similar response to shear as R1-19. For the R1-19 plasmid, we additionally confirmed the five-fold increase in the conjugation rate in separate experiments where the conjugation rate of a sample mixed

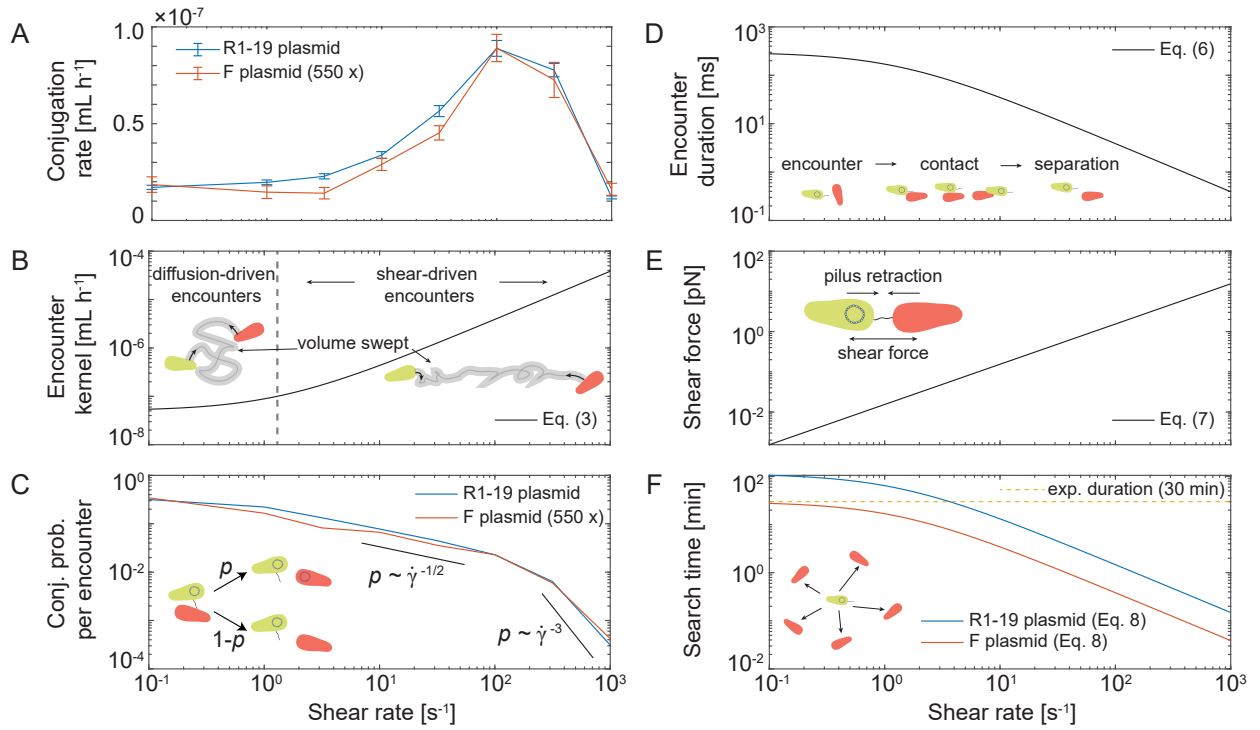


FIG. 2: Conjugation rate depends on the physical mechanisms that bring cells together and shear forces that separate cells. **A**, The observed conjugation rate vs. applied shear rate for two conjugative plasmids shared between two *E. coli* strains (pR1-19, blue, or F, orange; same data as in Fig. 1D). **B**, Encounter kernel vs. shear rate (Eq. 3). Diffusion dominates encounters at low shear rates ($\dot{\gamma} < 1.3 \text{ s}^{-1}$, broken vertical line; Eq. (4)), whereas shear is the primary encounter mechanism at higher shear rates. The insets are schematics of different trajectories in both regimes, with the grey line indicating the volume swept in each scenario. **C**, The probability of conjugation per cell-cell encounter vs. shear rate (Eq. 5). This probability is obtained by dividing the observed mean conjugation rate (A) by the theoretical encounter kernel (B). The probability decreases steadily until the optimal shear rate is reached, above which it decreases more rapidly, signaling the increasingly detrimental impact of shear on the mating process. The black auxiliary lines show two different scaling exponents for reference. **D**, Encounter duration vs. shear (Eq. 6). The theoretical duration that two cells are nearby is below a millisecond at the highest shear. **E**, Shear force on a mating pair vs. shear (Eq. 7). The theoretical shear force on a mating pair increases linearly with increasing shear. **F**, Estimated search time for a recipient vs. shear (Eq. 8). At low shear, a donor finds a recipient within a duration comparable to the experiment duration (30 min). At the highest shear ($\dot{\gamma} = 1 \times 10^3 \text{ s}^{-1}$), it takes several seconds for a donor to find a recipient.

at $\dot{\gamma} = 1 \times 10^2 \text{ s}^{-1}$ was compared with a simultaneous (rather than sequential) no-flow control (SI). To eliminate the possibility that the increase in the conjugation rate is driven not directly by shear but by heterogeneity in cell concentrations, we confirmed that cells mixed at $\dot{\gamma} = 1 \times 10^2 \text{ s}^{-1}$ remain homogeneously distributed in the rheometer at the end of mixing. This confirms that the overall encounter rate is not artificially inflated by local hotspots of high cell concentration (SI). Next, we explored the shear response of the conjugation rate in more detail.

To better understand the observed response of the conjugation rate to shear (Fig. 2A), we must assess how shear affects the probability of conjugation per encounter as well as the encounter kernel (compare Eq. 5). Considering the total encounter kernel (Eq. 3) as a function of the shear rate (Fig. 2B) demonstrates that encounters are driven by diffusion rather than shear at low shear

rates. Equating $\Gamma_{\text{diff}} = \Gamma_{\text{shear}}$ in Eq. (4), gives the shear rate $\dot{\gamma} = 1.3 \text{ s}^{-1}$ at which shear overtakes diffusion in determining the encounter rate (broken vertical line in Fig. 2B). This shear value is a close match to the observed transition from the conjugation plateau to the increase in conjugation rate with increasing shear rate.

Our results further reveal that the probability of conjugation per donor-recipient encounter decreases with increasing shear rate. Dividing the observed mean conjugation rate by the theoretical encounter kernel from Eq. (5) yields the experimentally observed probability of conjugation per donor-recipient encounter (Fig. 2C). We find that this probability decreases with increasing shear rate, suggesting that higher shear makes it harder for cells to form stable mating pairs. This is in line with previous observations in incubator shakers [26]. Above the observed optimal shear rate ($\dot{\gamma} \approx 1 \times 10^2 \text{ s}^{-1}$), the probability of conjugation per encounter decreases more steeply in re-

lation to the shear rate. In this range, the increase in the number of donor-recipient encounters through a higher shear rate is overtaken by the detrimental impact of shear on the conjugation process, leading to a decrease in the overall conjugation rate.

We hypothesize that the detrimental impact of shear at high shear rates arises either because cell-cell encounters are too short for cells to form mating pairs or because the shear forces acting on cells become so strong they can disrupt the mating process. The average encounter duration $t_{\text{encounter}}$ can be estimated as [35]

$$t_{\text{encounter}} = V_{\text{cell}}/\Gamma, \quad (6)$$

where $V_{\text{cell}} = 4/3\pi r^3$ is the cell volume (we take $r = 1 \mu\text{m}$ for both donors and recipients). This time (Fig. 2D) represents the time needed to sweep a volume equal to the cell volume. Based on this estimate, a donor-recipient encounter lasts approximately 0.3 s at low shear rates ($\dot{\gamma} = 1 \times 10^{-1} \text{ s}^{-1}$) and drops to 0.4 ms at the highest shear rate ($\dot{\gamma} = 1 \times 10^3 \text{ s}^{-1}$). Previous work showed that pilus extension and retraction each take about twenty seconds with an additional twenty seconds of lag time between the extension and retraction [10]. These timescales are longer than the encounter duration, which leaves increasingly little time for a pilus to attach to the surface of a recipient as the shear rate increases. Another mechanism that may hamper the plasmid transfer is the disruption of donor-recipient pairs that have already formed by the fluid shear forces. The magnitude of the hydrodynamic force acting upon two touching cells in a shear flow can be estimated as [36, 37]

$$f_{\text{shear}} = 6.12\pi\mu r^2\dot{\gamma}, \quad (7)$$

where μ is the dynamic viscosity of the liquid. With $r = 1 \mu\text{m}$ and $\mu = 0.8 \text{ mPa}\cdot\text{s}$, we find that the shear force acting on the connection between the two cells exceeds 10 pN at the highest shear rate ($\dot{\gamma} = 1 \times 10^3 \text{ s}^{-1}$, Fig. 2E). The polymerization machinery in type IV pili produces forces that can, for brief transients, reach 100 pN [38]. Similarly, force-extension measurements of F pili show that forces above 10 pN start to mechanically extend a pilus [27]. Thus, the decrease in the conjugation rate at the highest shear rate ($\dot{\gamma} = 1 \times 10^3 \text{ s}^{-1}$) may come from the shear forces partly preventing pilus retraction. Alternatively, even if the pilus manages to retract, the shear forces may still separate the mating cells during the subsequent plasmid transfer stage, which takes at least several minutes [9, 10]. At the highest shear rates reached in our experiment, the shear did not irreversibly damage the cells or pili. To test this, we performed conjugation experiments with the R1-19 plasmid where we first exposed cells to the highest shear rate used in our experiments ($\dot{\gamma} = 1 \times 10^3 \text{ s}^{-1}$) and then reverted back to the optimal shear rate ($\dot{\gamma} = 1 \times 10^2 \text{ s}^{-1}$). We compared the measured conjugation rates with a control experiment in which cells

were exposed only to the optimal shear rate (SI). These experiments showed that cells fully recovered the same maximal conjugation rate at the optimal shear rate after initial exposure to the higher shear rate. Overall, several mechanisms, such as short encounter duration, which prevents mating pair formation, and high shear forces, which interrupt pilus retraction or separate mating pairs, may drive the drop in conjugation rate observed at high shear rates.

The duration of the conjugation event, rather than the search time, likely limits the maximum conjugation rate in our experiments. From the perspective of a single donor cell, it takes on average a ‘search time’ [11, 28]

$$t_{\text{search}} = (\Gamma c_{\text{R}})^{-1}, \quad (8)$$

to encounter a recipient cell. This time is displayed in Fig. 2F for the recipient concentrations used in our experiments ($c_{\text{R}} = 1.05 \times 10^7 \text{ mL}^{-1}$ for R1-19 and $c_{\text{R}} = 4.02 \times 10^7 \text{ mL}^{-1}$ for F). The search time is of the same order as the experiment duration (30 min) at low shear rates and drops to several seconds at the highest shear rates. Thus, donor cells have very frequent encounters with recipient cells at high shear rates, whereas only a single donor-recipient interaction typically happens at low shear. Given that conjugation lasts at least several minutes [9, 10], this estimate implies that the observed peak conjugation rate may be limited not by the search time but by the conjugation duration. Namely, donors may find a viable conjugation partner fast at the optimal shear rate and then spend the remaining time conjugating and are thus able to repeat the whole cycle at most a handful of times during the experiment. In a more dilute system, or when only a small subpopulation of cells represent viable recipients (e.g., due to phylogenetic distance [18] or the presence of compatible mating pair stabilization mechanisms [39]), cells may be limited by the search time at all shear rates. In such scenarios, we expect that the maximum enhancement in the conjugation rate due to shear over diffusion alone will be even higher than the factor of five observed here.

Connecting laboratory measurements of conjugation rates with environmentally relevant conditions is important to constraint horizontal gene transfer rates in the environment [1, 40]. Our experimental conditions most closely mimic mixing in aquatic environments due to the relatively low cell densities ($\sim 10^7 \text{ mL}^{-1}$) in a low-viscosity condition (LB medium). Marine environments host diverse microbiota [41] that experience vastly different turbulence (and thus shear) levels as a function of depth in the water column [12, 42]. We next use our experimental observations to quantify the effect of shear on conjugation rates at different depths in the ocean.

Turbulence in the ocean’s surface waters may elevate the conjugation rate compared to more quiescent deeper

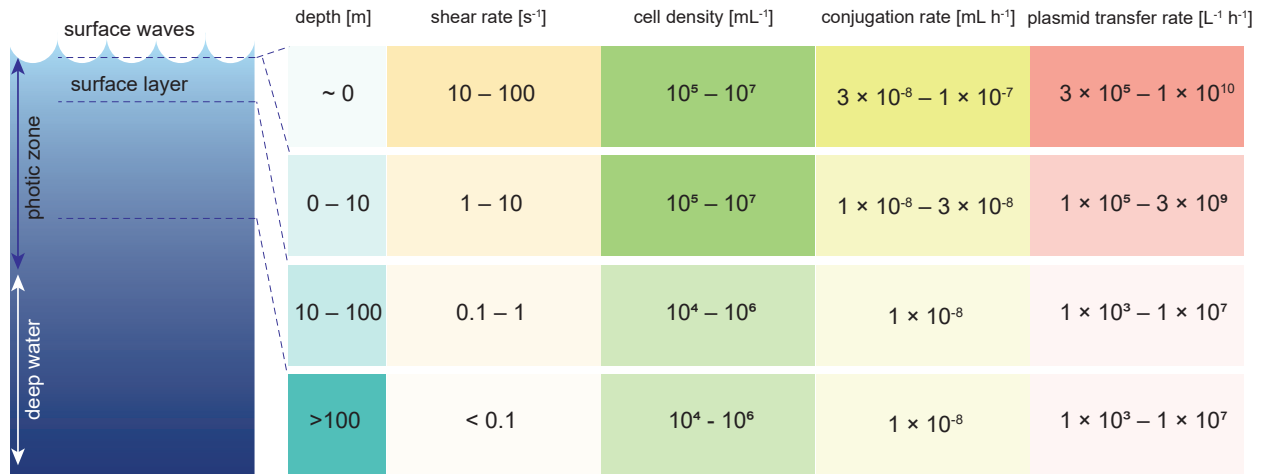


FIG. 3: **Ocean surface layer and breaking waves as conjugation hotspots.** The schematic shows estimates of the conjugation rate and the number of plasmid transfers per volume per time at different depths in the ocean based on the combination of the experimental results shown in Fig. 1D and observational data of shear rates and cell densities in the ocean (see Eq. (10)).

waters, with breaking waves acting as a conjugation hotspot (Fig. 3). We map the mean encounter rate experienced by cells in our experiments onto the mean encounter rate in turbulence as follows. Bacteria are much smaller than the Kolmogorov scale, the smallest scale in a turbulent flow [43], which in the ocean is typically in the range 1-6 mm [44]. At such small scales, the encounter kernel characterizing cell-cell encounters is [45]

$$\Gamma_{\text{turb}} = 1.3(r_D + r_R)^3 \sqrt{\epsilon/\nu}, \quad (9)$$

where ϵ is the kinetic energy dissipation rate and ν is the kinematic viscosity of water. The kernel in Eq. (9) is identical with the kernel Γ_{shear} in Eq. (4a) to within 3%, when one uses the turbulent shear rate $\dot{\gamma} = \sqrt{\epsilon/\nu}$. Based on this similarity between the kernels, we assume that the probability of conjugation per encounter p has the same dependence on shear as in our experiments, which enables us to map the environmental shear levels on the measured conjugation rate. Below ten meters, turbulent shear rates are typically low ($\dot{\gamma} < 1 \text{ s}^{-1}$) [12], which corresponds to the diffusion-dominated regime with cell-cell encounters driven by Brownian motion (our experiments' low-shear plateau). Hence, to model a plasmid spreading in deeper waters ($> 10 \text{ m}$), we take $\eta \approx 1 \times 10^{-8} \text{ mL h}^{-1}$ for the R1-19 plasmid (the value for the plateau in Fig. 1D). Conversely, the shear rate in the top ten meters is in the range $\dot{\gamma} \approx 1 - 10 \text{ s}^{-1}$, and breaking waves can generate $\dot{\gamma} \approx 100 \text{ s}^{-1}$ [42]. Thus, we assume $\eta \approx 1 \times 10^{-8} - 3 \times 10^{-8} \text{ mL h}^{-1}$ in the top ten meters and the extreme $\eta \approx 1 \times 10^{-7} \text{ mL h}^{-1}$ in breaking waves (peak value in Fig. 1D). The extremely high shear rate of $\dot{\gamma} \approx 1 \times 10^3 \text{ s}^{-1}$ is rarely, if ever, observed, implying that ocean turbulence is too weak to disrupt conjugation mechanically. Based on a global survey of

microbial abundances, we take cell concentrations in the range $c \approx 1 \times 10^5 - 1 \times 10^7 \text{ mL}^{-1}$ in the top 100 m and $c \approx 1 \times 10^4 - 1 \times 10^6 \text{ mL}^{-1}$ below 100 m [13]. Combining these estimates, we compute the plasmid transfer rate per liter per hour as a function of depth z as follows

$$\text{plasmid transfer rate} \approx \eta[\dot{\gamma}(z)]c^2(z). \quad (10)$$

Fig. 3 summarizes our estimates and suggests that breaking waves could act as conjugation hotspots based on the combination of high cell concentrations and a strong enhancement of the conjugation rate by turbulent shear.

To assess the importance of conjugation between members of a phylogenetically related marine community, we compare the plasmid transfer rate among *Roseobacters* against the spontaneous mutation rate, which occurs during DNA replication. Conjugation rates, in general, depend on phylogeny [7, 18]. If only a fraction β of cells participates in conjugation, then the estimates in Fig. 3 decrease by a factor of β^2 . We consider the *Roseobacter* clade, which is found predominantly in marine environments, representing up to 20% ($\beta = 0.2$) of bacterial cells in some coastal ecosystems and 3 to 5% ($\beta = 0.03 - 0.05$) of bacterial cells in open ocean surface waters [46]. A recent analysis revealed the existence of mobilizable marine plasmids capable of spreading into diverse members of the *Roseobacter* group [5, 47]. To compare the plasmid transfer rate with the spontaneous mutation rate, we assume cells divide once per day and mutate spontaneously at a rate of 2.5×10^{-3} mutations per genome per replication [48]. We find that the plasmid transfer rate is larger than the spontaneous mutation rate across a wide range of environmentally relevant cell concentrations (SI). For example, assuming a large total cell con-

centration ($1 \times 10^6 \text{ mL}^{-1}$), Roseobacters representing a large fraction of the population ($\beta = 0.1$), and taking $\eta \approx 1 \times 10^{-7} \text{ mL h}^{-1}$ for the conjugation rate in the surface ocean, the plasmid transfer rate is two orders of magnitude higher than the spontaneous mutation rate (see SI for a detailed calculation). These estimates indicate that conjugation in the turbulent surface ocean has the potential to generate faster genetic adaptation in marine bacteria than spontaneous mutations.

Discussion

We have performed bacterial conjugation experiments under controlled shear conditions. While previous experiments suggested an important role for fluid shear in controlling conjugation efficiency [25–27], they were based on conventional laboratory shakers. Flows in such shakers are difficult to characterize, preventing a quantitative and mechanistic understanding of the opposing role of shear on conjugation, which can act to increase the conjugation rate by increasing cell-cell encounters but can also disrupt the mating pairs. We have overcome this limitation by quantifying conjugation rates within a cone and plate rheometer, which creates a controlled shear flow and, thus, a controlled donor-recipient encounter rate. We discovered that the conjugation rate increases with shear until it peaks at an optimal shear rate, reaching a value five-fold higher than the baseline set by diffusion-driven encounters. The precise control over cell-cell encounters in the rheometer combined with encounter rate theory enabled us to map out the conjugation rate as a function of depth in a marine environment. Consequently, we predicted that the ocean surface waves could act as hotspots of conjugation by generating high enough shear to increase cell-cell encounters without impairing conjugation and that conjugation can drive faster genetic adaptation than spontaneous mutation. More broadly, our results indicate that environmental flows could locally increase conjugation rates in aquatic systems, gut, and soil.

The dependence of the conjugation rate on shear for the two plasmids we tested, R1-19 and F, was very similar upon a simple rescaling (Fig. 1D). It remains to be seen whether this shear dependence holds universally across different species and plasmid types. Plasmids used in this study belong to the IncF incompatibility class, which produce long, flexible, and retractable pili [8, 49]. Plasmids in the IncW or IncP incompatibility classes produce short, rigid pili, conjugate poorly in liquids, and require surfaces to support mating [49]. For such plasmids, we expect that the optimal conjugation rate occurs at much lower shear rates than for plasmids in the IncF class. Conversely, the stickiness mediated by the presence of compatible mating pair stabilization protein complexes [39] may enable mating pairs to withstand higher shear.

Motility can generate more donor-recipient encounters

than diffusion or turbulence. In our experiments, motility did not play a prominent role because we deliberately used a nonmotile recipient and only a small subpopulation of donors was moderately motile (SI). However, the encounter kernel $\Gamma_{\text{swim}} = \pi(r_D + r_R)^2 U_{\text{swim}}$ characterizing encounters between swimming cells [11] implies that a population of cells swimming at speed $U_{\text{swim}} = 10 \mu\text{m s}^{-1}$ generates as many cell-cell encounters as a shear rate $\dot{\gamma} = 10 \text{ s}^{-1}$ corresponding to strong turbulence. Because up to 10% of bacteria can be motile in coastal waters [50], motility could be an important phenotype boosting conjugation in motile subpopulations.

Constraining horizontal gene transfer rates in natural settings is important for identifying bottlenecks and drivers of microbial evolution, including antibiotic resistance spread [7, 40, 51]. Our assay allows for the direct control of cell-cell encounters in conjugation experiments, which enables the factorization of the observed conjugation rate into the physical encounter rate and the probability of conjugation per donor-recipient encounter (Eq. 5, Fig. 2C). Predicting conjugation rates in other scenarios is then possible by multiplying the probability by the encounter kernel characterizing encounters in the new scenario.

In summary, we used a cone and plate rheometer as a ‘cell collider’ and performed conjugation experiments between *E. coli* sharing conjugative plasmids while controlling cell-cell encounters. We found that fluid shear does not impact conjugation at low shear rates because diffusion drives cell-cell encounters in this regime. As shear increases, the conjugation rate increases, boosting the conjugation rate approximately five-fold at an optimal shear rate of $\dot{\gamma} \approx 1 \times 10^2 \text{ s}^{-1}$. At higher shear rates than this, shear hampers conjugation either because it prevents the formation of mating pairs or mechanically disrupts that mating process. Because fluid flows are widely present in aquatic, gut, and soil environments, and the associated shear rates span orders of magnitude [12, 15, 16], our results suggest that shear could induce hotspots of bacterial conjugation in the environment.

Acknowledgements

We gratefully acknowledge funding from a Human Frontier Science Program (HFSP) Postdoctoral Fellowship LT0045/2023-L to J.S.H.; a Gordon and Betty Moore Foundation Symbiosis in Aquatic Systems Initiative Investigator Award (GBMF9197), the Simons Foundation through the Principles of Microbial Ecosystems (PriME) collaboration (grant 542395FY22), Swiss National Science Foundation grant 205321_207488, Swiss National Science Foundation Sinergia grant CRSII5-186422, and the Swiss National Science Foundation, National Centre of Competence in Research (NCCR) Microbiomes (No. 51NF40_180575) to R.S.; and a Swiss National Science Foundation Ambizione grant no. PZ00P2_202188 to J.S.

This research was supported in part by the National Science Foundation under PHY-2309135.

We thank Deepthi Vinod and David Johnson for providing us with the donor strain with the two plasmids and Roberto Pioli for providing us with the recipient strain. We thank Yao Zhou for the initial assistance, and Uria Alcolombri and Sebastian Bonhoeffer for discussions.

Figures were partly generated using Servier Medical Art, provided by Servier, licensed under a Creative Commons Attribution 3.0 unported license.

Materials and Methods

Bacterial strains: As a plasmid donor, we used the *Escherichia coli* strain TB204 Δ trpC-GFP, a derivative of the strain MG1655 made auxotroph for tryptophan and fluorescently labeled with the fluorophore sfGFP on the chromosome [52]. In our experiments, the strain carried one of two different plasmids. The first one is the R1-19 plasmid, a self-mobilizable, derepressed, and up-regulated variant of the R1 plasmid that also contains a resistance gene against chloramphenicol [53]. The second plasmid Ftet is a variant of the F-plasmid [54] containing an additional resistance gene against tetracycline. As a recipient strain, we used a Δ motA mutant of the strain NCM3722 [55], which lacks flagella and is non-motile. Furthermore, we had used mini-Tn7 insertion [56] to chromosomally tag this strain with the fluorophore dsRed and a resistance gene against gentamicin. The insertion (pUC18T-mini-Tn7T-Gm-dsRedExpress; Addgene #65032) and the helper plasmid (pTNS1; Addgene #64967) were a gift from Herbert Schweizer.

Media preparation: A standard Luria broth (subsequently called LB; Miller; product name: DifcoTM LB Broth, Miller (Luria-Bertani) from Becton, Dickinson and Company) was used as medium for both culturing and the conjugation experiments. At some stages (as specified below) antibiotics were added to that broth.

Culture preparation: Cultures of one of the donors strains and of the recipient were grown over night with shaking at 200 rpm at 30 °C in LB medium containing one of the following antibiotics: 25 $\mu\text{g mL}^{-1}$ chloramphenicol (R1-19), 10 $\mu\text{g mL}^{-1}$ tetracycline (F), respectively 30 $\mu\text{g mL}^{-1}$ gentamicin (recipient). On the next day, samples of these cultures were 100x diluted in fresh LB containing the same antibiotics at the same concentrations and further incubated at 30 °C with shaking at 200 rpm for 2 h to ensure the cells were in the exponential growth phase. Thereafter, these cultures were centrifuged down with 2000 g at 25 °C for 10 min to replace the supernatant with LB free of antibiotics. In the same process, the newly formed cell suspensions were diluted to make their OD600 match a specific value (0.05 for R1-19 as donor,

0.20 for F as donor). These cell suspensions were then split into eight pairs of donor and recipient aliquots, one pair for each individual assay of the day. Each assay was later exposed to a different shear rate in the rheometer. Until they were being used in the rheometer, these aliquots were stored at 4 °C in a fridge. We observed no significant growth in these aliquots during that time (SI). To determine the initial concentrations of donors and recipients, samples of 15 μL were taken from the aliquots prepared for the first and last assay of the day, and the cell density in these samples was measured using a hemacytometer (Bright-Line, Hauser Scientific).

Shear-flow driven conjugation assay: For each individual assay, from one aliquot of the donor and one of the recipient equal amounts were mixed and vortexed for 10 s to create a homogeneously mixed donor-recipient cell suspension. Of this mixture, 1.2 mL were loaded onto the rheometer (Kinexus lab+ by NETZSCH, #KNX2112) that had been pre-warmed to a temperature of 30 °C by its Peltier plate temperature control module (NETZSCH #KNX2001-E) and heat exchanger (NETZSCH #KNX2500). Then the upper, cone-shaped geometry (4° angle; NETZSCH #NX2036) was lowered down onto the liquid, the moisture trap was closed around it and the liquid was getting consistently and accurately stirred at the desired shear rate for 30 min at a stable temperature of 30 °C.

Each of the eight individual assays was exposed to a different shear rate: we sequentially scanned eight shear rates from low ($\dot{\gamma} = 1 \times 10^{-1} \text{ s}^{-1}$) to high ($\dot{\gamma} = 1 \times 10^3 \text{ s}^{-1}$) or from high to low on any given day. For each plasmid, we repeated each experiment four times on different days (two up-ramps and two down-ramps).

Transconjugant quantification via time to threshold: After the stirring came to an end, the cone-shaped upper geometry was gently raised and a sample was taken from the cell suspension in the rheometer (200 μL if R1-19 was the donor; 400 μL if F was the donor). This sample was diluted in a selective medium: 1800 μL (R1-19, 10x dilution) respectively 1600 μL (F, 5x dilution) of LB cooled down at 4 °C containing both 30 $\mu\text{g mL}^{-1}$ gentamicin as well as either 25 $\mu\text{g mL}^{-1}$ chloramphenicol (R1-19) or 10 $\mu\text{g mL}^{-1}$ tetracycline (F). After that, this mixture was vortexed for 5 s. The dilution of the sample was performed to reduce the encounter rate due to diffusion and thus the number of possible post-mixing conjugation events, the exposure to cold temperature was used to suppress the growth of the transconjugants, the only cell type that is able to grow in this environment with both antibiotics present. These diluted samples were stored at 4 °C in a fridge, until the last experiment of that day's series had been performed (maximal time in the fridge: approximately 5 h). Then, volumes of 200 μL of these diluted samples were loaded into wells on a 96 well plate.

Normally, 8-9 technical replicates were made from the sample of each assay, depending on available space on the plate. In addition, 16 wells on the plate were allocated to perform positive and negative controls, including the quantification of the number of additional transconjugants formed after the actual assay, which was negligible (SI). After loading, the OD600 of all the wells on the 96 well plate were measured in intervals of 5 min for the next 24-72 h using an automated plate reader (BioTek Synergy H1 by Agilent and BioTek Synergy HTX by Agilent). The so measured growth curves were transformed into initial concentrations of transconjugants by applying the time to threshold method established by Bethke et al. [23] for which we prepared our own calibration curve (SI).

Data analysis: To calculate the conjugation rate at a given shear rate, we used Eq. (1). For the endpoint transconjugant concentration $c_T(t_m)$, we used the average over individual transconjugant concentrations measured in the different technical replicates of an individual conjugation assay at a given shear rate. Each technical replicate corresponded to a cell concentration obtained by converting OD600 readouts from individual wells in the 96 well plate to cell concentrations using the calibration curve of the time to threshold method. For the error of $c_T(t_m)$, we computed the standard error of the mean over the individual technical replicates. The average initial concentrations of donors $c_D(0)$ and recipients $c_R(0)$, together with their respective standard errors, were determined at the end of the culture preparation (SI). The mating duration t_m , the duration of an individual assay, was always 30 min. We computed the average conjugation rate according to Eq. (1) using the average values of $c_T(t_m)$, $c_D(0)$ and $c_R(0)$ described above. The error of the conjugation rate follows from error propagation of the measured standard errors. Since for both plasmids there were four independent series of assays on four different days and, hence, at each shear rate four independent biological replicates measuring the conjugation rate at that shear rate, the average over these four conjugation rates was calculated as the final estimate of the conjugation rate and is displayed in Fig. 1D. Its error was determined from the errors of the individual measurements of the conjugation rate using the laws of error propagation (SI).

-
- [1] R. I. Aminov, "Horizontal gene exchange in environmental microbiota," *Frontiers in Microbiology*, vol. 2, pp. 1–19, 2011.
- [2] C. M. Thomas and K. M. Nielsen, "Mechanisms of, and barriers to, horizontal gene transfer between bacteria," *Nature Reviews Microbiology*, vol. 3, pp. 711–721, 2005.
- [3] S. M. Soucy, J. Huang, and J. P. Gogarten, "Horizontal gene transfer: Building the web of life," *Nature Reviews*

- Genetics*, vol. 16, pp. 472–482, 2015.
- [4] Y. Nakamura, T. Itoh, H. Matsuda, and T. Gojobori, "Biased biological functions of horizontally-transferred genes in prokaryotic genomes," *Nature Genetics*, vol. 36, pp. 760–766, 2004.
- [5] J. Petersen, J. Vollmers, V. Ringel, H. Brinkmann, C. Ellebrandt-Sperling, C. Spröer, A. M. Howat, J. C. Murrell, and A. K. Kaster, "A marine plasmid hitchhiking vast phylogenetic and geographic distances," *Proceedings of the National Academy of Sciences of the U. S. A.*, vol. 116, pp. 20568–20573, 2019.
- [6] E. Bakkeren, J. S. Huisman, S. A. Fattinger, A. Hausmann, M. Furter, A. Egli, E. Slack, M. E. Sellin, S. Bonhoeffer, R. R. Regoes, M. Diard, and W. D. Hardt, "Salmonella persists promote the spread of antibiotic resistance plasmids in the gut," *Nature*, vol. 573, pp. 276–280, 2019.
- [7] S. Castañeda-Barba, E. M. Top, and T. Stalder, "Plasmids, a molecular cornerstone of antimicrobial resistance in the One Health era," *Nature Reviews Microbiology*, vol. 22, pp. 18–32, 2024.
- [8] D. Arutyunov and L. S. Frost, "F conjugation: back to the beginning," *Plasmid*, vol. 70, pp. 18–32, 2013.
- [9] A. Babić, A. B. Lindner, M. Vulić, E. J. Stewart, and M. Radman, "Direct visualization of horizontal gene transfer," *Science*, vol. 319, pp. 1533–1536, 2008.
- [10] K. Goldlust, A. Ducret, M. Halte, A. Dedieu-Berne, M. Erhardt, and C. Lesterlin, "The F pilus serves as a conduit for the DNA during conjugation between physically distant bacteria," *Proceedings of the National Academy of Sciences of the U. S. A.*, vol. 120, p. e2310842120, 2023.
- [11] J. Slomka, U. Alcolombri, F. Carrara, R. Foffi, F. J. Peaudecerf, M. Zbinden, and R. Stocker, "Encounter rates prime interactions between microorganisms," *Interface Focus*, vol. 13, p. 20220059, 2023.
- [12] P. J. Franks, B. G. Inman, J. A. MacKinnon, M. H. Alford, and A. F. Waterhouse, "Oceanic turbulence from a planktonic perspective," *Limnology and Oceanography*, vol. 67, pp. 348–363, 2022.
- [13] C. H. Wigington, D. Sonderegger, C. P. Brussaard, A. Buchan, J. F. Finke, J. A. Fuhrman, J. T. Lennon, M. Middelboe, C. A. Suttle, C. Stock, W. H. Wilson, K. E. Wommack, S. W. Wilhelm, and J. S. Weitz, "Re-examination of the relationship between marine virus and microbial cell abundances," *Nature Microbiology*, vol. 1, pp. 1–9, 2016.
- [14] J. Cremer, I. Segota, C. Yang, M. Arnoldini, J. T. Sauls, Z. Zhang, E. Gutierrez, A. Groisman, and T. Hwa, "Effect of flow and peristaltic mixing on bacterial growth in a gut-like channel," *Proceedings of the National Academy of Sciences of the U. S. A.*, vol. 113, pp. 11414–11419, 2016.
- [15] D. L. Kurz, E. Secchi, F. J. Carrillo, I. C. Bourg, R. Stocker, and J. Jimenez-Martinez, "Competition between growth and shear stress drives intermittency in preferential flow paths in porous medium biofilms," *Proceedings of the National Academy of Sciences of the U. S. A.*, vol. 119, p. e2122202119, 2022.
- [16] M. Schütt, C. O'Farrell, K. Stamatopoulos, C. L. Hoad, L. Marciani, S. Sulaiman, M. J. H. Simmons, H. K. Batchelor, and A. Alexiadis, "Simulating the hydrodynamic conditions of the human ascending colon: a digital twin of the dynamic colon model," *Pharmaceutics*,

- vol. 14, p. 184, 2022.
- [17] J. Lederberg and E. L. Tatum, "Gene recombination in *Escherichia coli*," *Nature*, vol. 158, p. 45, 1946.
- [18] R. J. Sheppard, A. E. Beddis, and T. G. Barraclough, "The role of hosts, plasmids and environment in determining plasmid transfer rates: A meta-analysis," *Plasmid*, vol. 108, p. 102489, 2020.
- [19] B. R. Levin, F. M. Stewart, and V. A. Rice, "The kinetics of conjugative plasmid transmission: Fit of a simple mass action model," *Plasmid*, vol. 2, pp. 247–260, 1979.
- [20] J. S. Huisman, F. Benz, S. J. Duxbury, J. A. G. de Visser, A. R. Hall, E. A. Fischer, and S. Bonhoeffer, "Estimating plasmid conjugation rates: A new computational tool and a critical comparison of methods," *Plasmid*, vol. 121, p. 102627, 2022.
- [21] O. Kosterlitz and J. S. Huisman, "Guidelines for the estimation and reporting of plasmid conjugation rates," *Plasmid*, vol. 126, p. 102685, 2023.
- [22] A. J. Lopatkin, S. Huang, R. P. Smith, J. K. Srimani, T. A. Sysoeva, S. Bewick, D. K. Karig, and L. You, "Antibiotics as a selective driver for conjugation dynamics," *Nature Microbiology*, vol. 1, pp. 1–8, 2016.
- [23] J. H. Bethke, A. Davidovich, L. Cheng, A. J. Lopatkin, W. Song, J. T. Thaden, V. G. Fowler Jr, M. Xiao, and L. You, "Environmental and genetic determinants of plasmid mobility in pathogenic *Escherichia coli*," *Science advances*, vol. 6, p. eaax3173, 2020.
- [24] L. Simonsen, D. M. Gordon, F. M. Stewart, and B. R. Levin, "Estimating the rate of plasmid transfer: an endpoint method," *Journal of General Microbiology*, vol. 136, pp. 2319–2325, 1990.
- [25] M. Clarke, L. Maddera, R. L. Harris, and P. M. Silverman, "F-pili dynamics by live-cell imaging," *Proceedings of the National Academy of Sciences of the U. S. A.*, vol. 105, pp. 17978–17981, 2008.
- [26] X. Zhong, J. E. Krol, E. M. Top, and S. M. Krone, "Accounting for mating pair formation in plasmid population dynamics," *Journal of Theoretical Biology*, vol. 262, pp. 711–719, 2010.
- [27] J. B. Patkowski, T. Dahlberg, H. Amin, D. K. Gahlot, S. Vijayarajratnam, J. P. Vogel, M. S. Francis, J. L. Baker, M. Andersson, and T. R. Costa, "The F-pilus biomechanical adaptability accelerates conjugative dissemination of antimicrobial resistance and biofilm formation," *Nature Communications*, vol. 14, p. 1879, 2023.
- [28] T. Kjørboe, *A mechanistic approach to plankton ecology*. Princeton University Press, 2008.
- [29] A. B. Burd and G. A. Jackson, "Particle aggregation," *Annual Review of Marine Science*, vol. 1, pp. 65–90, 2009.
- [30] M. Smoluchowski, "Drei Vorträge über Diffusion, Brownsche Bewegung und Koagulation von Kolloidteilchen," *Physikalische Zeitschrift*, vol. 17, pp. 557–599, 1916.
- [31] M. E. Fewell and J. D. Hellums, "The secondary flow of Newtonian fluids in cone-and-plate viscometers," *Transactions of the Society of Rheology*, vol. 21, pp. 535–565, 1977.
- [32] H. P. Sdougos, S. R. Bussolari, and C. F. Dewey, "Secondary flow and turbulence in a cone-and-plate device," *Journal of Fluid Mechanics*, vol. 138, pp. 379–404, 1984.
- [33] T. Kjørboe, K. P. Andersen, and H. G. Dam, "Coagulation efficiency and aggregate formation in marine phytoplankton," *Marine Biology*, vol. 107, pp. 235–245, 1990.
- [34] K. S. Mead and M. W. Denny, "The effects of hydrodynamic shear stress on fertilization and early development of the purple sea urchin *Strongylocentrotus purpuratus*," *The Biological Bulletin*, vol. 188, pp. 46–56, 1995.
- [35] J. M. Hutchinson and P. M. Waser, "Use, misuse and extensions of "ideal gas" models of animal encounter," *Biological Reviews*, vol. 82, pp. 335–359, 2007.
- [36] S. L. Goren, "The hydrodynamic forces on touching spheres along the line of centers exerted by a shear field," *Journal of Colloid and Interface Science*, vol. 36, pp. 94–96, 1971.
- [37] J. C. Husband and J. M. Adams, "Shear-induced aggregation of carboxylated polymer latices," *Colloid & Polymer Science*, vol. 270, pp. 1194–1200, 1992.
- [38] A. J. Merz, M. So, and M. P. Sheetz, "Pilus retraction powers bacterial twitching motility," *Nature*, vol. 407, pp. 98–102, 2000.
- [39] W. W. Low, J. L. Wong, L. C. Beltran, C. Seddon, S. David, H.-S. Kwong, T. Bizeau, F. Wang, A. Peña, T. R. Costa, *et al.*, "Mating pair stabilization mediates bacterial conjugation species specificity," *Nature Microbiology*, vol. 7, pp. 1016–1027, 2022.
- [40] D. G. Larsson and C.-F. Flach, "Antibiotic resistance in the environment," *Nature Reviews Microbiology*, vol. 20, pp. 257–269, 2022.
- [41] S. Sunagawa, L. P. Coelho, S. Chaffron, J. R. Kultima, K. Labadie, G. Salazar, B. Djahanschiri, G. Zeller, D. R. Mende, A. Alberti, *et al.*, "Structure and function of the global ocean microbiome," *Science*, vol. 348, p. 1261359, 2015.
- [42] P. Sutherland and W. K. Melville, "Field measurements of surface and near-surface turbulence in the presence of breaking waves," *Journal of Physical Oceanography*, vol. 45, pp. 943–965, 2015.
- [43] S. A. Thorpe, *An introduction to ocean turbulence*, vol. 10. Cambridge University Press Cambridge, 2007.
- [44] J. R. N. Lazier and K. H. Mann, "Turbulence and the diffusive layers around small organisms," *Deep Sea Research Part A. Oceanographic Research Papers*, vol. 36, pp. 1721–1733, 1989.
- [45] P. G. Saffman and J. S. Turner, "On the collision of drops in turbulent clouds," *Journal of Fluid Mechanics*, vol. 1, pp. 16–30, 1956.
- [46] M. A. Moran, R. Belas, M. A. Schell, J. M. González, F. Sun, S. Sun, B. J. Binder, J. Edmonds, W. Ye, B. Orcutt, *et al.*, "Ecological genomics of marine *Roseobacters*," *Applied and environmental microbiology*, vol. 73, pp. 4559–4569, 2007.
- [47] J. Petersen and I. Wagner-Döbler, "Plasmid Transfer in the Ocean—A Case Study from the *Roseobacter* group," *Frontiers in microbiology*, vol. 8, p. 1350, 2017.
- [48] J. W. Drake, B. Charlesworth, D. Charlesworth, and J. F. Crow, "Rates of spontaneous mutation," *Genetics*, vol. 148, pp. 1667–1686, 1998.
- [49] D. E. Bradley, D. Taylor, and D. Cohen, "Specification of surface mating systems among conjugative drug resistance plasmids in *Escherichia coli* K-12," *Journal of Bacteriology*, vol. 143, pp. 1466–1470, 1980.
- [50] J. G. Mitchell, L. Pearson, A. Bonazinga, S. Dillon, H. Khouri, and R. Paxinos, "Long lag times and high velocities in the motility of natural assemblages of marine bacteria," *Applied and environmental microbiology*, vol. 61, pp. 877–882, 1995.
- [51] M. J. Shepherd, T. Fu, N. E. Harrington, A. Kottara, K. Cagney, J. D. Chalmers, S. Paterson, J. L. Fothergill, and M. A. Brockhurst, "Ecological and evo-

- lutionary mechanisms driving within-patient emergence of antimicrobial resistance,” *Nature Reviews Microbiology*, vol. 22, pp. 650–665, 2024.
- [52] A. D. Co, S. van Vliet, D. J. Kiviet, S. Schlegel, and M. Ackermann, “Short-range interactions govern the dynamics and functions of microbial communities,” *Nature ecology & evolution*, vol. 4, pp. 366–375, 2020.
- [53] E. Meynell and N. Datta, “Mutant drug resistant factors of high transmissibility,” *Nature*, vol. 214, pp. 885–887, 1967.
- [54] L. L. Cavalli, J. Lederberg, and E. M. Lederberg, “An infective factor controlling sex compatibility in bacterium coli,” *Microbiology*, vol. 8, pp. 89–103, 1953.
- [55] S. Taheri-Araghi, S. Bradde, J. T. Sauls, N. S. Hill, P. A. Levin, J. Paulsson, M. Vergassola, and S. Jun, “Cell-size control and homeostasis in bacteria,” *Current biology*, vol. 25, pp. 385–391, 2015.
- [56] K.-H. Choi and H. P. Schweizer, “mini-Tn 7 insertion in bacteria with single att Tn 7 sites: example *Pseudomonas aeruginosa*,” *Nature protocols*, vol. 1, pp. 153–161, 2006.